Model-free feedback design for a Mixed Cancer Therapy

S. Chareyron and M. Alamir

CNRS/GIPSA-Lab /University of Grenoble, BP 46, Domaine Universitaire, rue de la Houille Blanche, 38400 Saint Martin d'Hères, France.
Tel.: +33 476 826 326, Fax: +33 476 826 388

abstract

In this paper a model-free feedback control design is proposed for the drug administration in mixed cancer therapy. This strategy is very attractive because of the important issue of parameter uncertainties unavoidable when dealing with biological models. The proposed feedback scheme use past measurements to update an on-line simplified model. The control design is then based on model predictive control in which a suitable switching is performed between two different cost functions. The effectiveness of the proposed model-free control strategy is validated using a recently developed model (unknown to the controller) governing the cancer growth on a cells population level under combined immune and chemotherapy and using real human data.

Keywords: Model-free strategy, control design, predictive control, mixed cancer therapy (chemotherapy-immunotherapy).

1 Introduction

The optimal way to administer drugs in cancer treatment by combining chemotherapy and immunotherapy remains an open

issue. A first reason lies in the lack of unified mathematical models for the underlying dynamics [10,18,23,20,19]. Indeed, models vary depending on the type of cancer and the family of drugs being used. Another difficulty comes from the variability of the model's parameters that can range up to more than 200% from one patient to another.

Several solutions have been explored in order to overcome these difficulties. For specific types of cancer described by simple models, it has been possible to propose treatment strategies that are based on the identification for each patient of its own set of parameters. This method applied to treat breast cancer for clinical trials already reveals interesting perspectives [2]. However, many other types of cancer are described by models of high complexity (involving different time and space scales) described through a large number of parameters. In these situations, the identification of the set of parameters for each patient may become a difficult task. Indeed, it is a well-known fact in identification theory that when a system is described by a large number of parameters, the problem might be ill-conditioned unless the identification is realized under extremely rich excitation signals. Unfortunately, this is impossible to do in cancer treatment where the identification would have been performed under the on-line treatment signals that are generally insufficient to guarantee good identifiability of the model parameters. In a recent work [5], it has been shown that one can avoid identifying a large number of parameters by concentrating on their key effect on the tumor cells dynamics. Coupled with this low order on-line identification scheme, a Nonlinear Model Predictive Control (NMPC) [1] has been used and robustness against parameter uncertainties has been investigated. The results showed nice properties as long as the uncertainties remained reasonably bounded. More precisely, for real-life uncertainties, the choice of the nominal values of parameters may be critical.

This paper aims at providing a new general treatment strategy that is no longer based on a before-hand given physiological model. Instead, a linear regression is adapted on-line (based on

past cells population measurements) in order to obtain a short-term predictive model that can be used in NMPC feedback design. Moreover, since the relevance of the identified model may depend on the length of the prediction horizon being used, a measurement based adaptation of the prediction horizon is also proposed.

The proposed feedback scheme is validated through simulations. The evolution of the patient cells population is are simulated using a recently developed model governing the cancer growth on a cells population level with combination of immune and chemotherapy [6,7,5]. This model used in the simulations is not known to the controller that uses exclusively the measurement-based model as described above. The choice of this model is justified by the fact that it exhibits qualitative phenomenon clinically observed such as tumor dormancy, oscillation in tumor size as well as bifurcation-like behavior. Note that in [6,7], the effects of the parameters variability is clearly illustrated by the fact that identical open-loop injection profiles can be successful for one patient and inadequate for another even when starting from the same initial state. This perfectly illustrates the relevance of model free solutions as the one proposed in the present contribution.

The paper is organized as follows: First, the model of [6,5,7] is briefly described (section 2). Then, the formulations of optimal control problems for mixed (immunotherapy chemotherapy) therapy is described (section 3), and the proposed feedback strategy is explained (section 4). Finally, illustrating simulations are proposed in section 5.

2 Notations and dynamical evolution of key cells populations

In this section, the model proposed by [6,7] that is used in the validating simulations is briefly described.

This model involves the following cell populations:

- T: tumor cells population.
- N: total NK cells population. These cells are part of the innate immune system and therefore exist even when no tumor cells are present [6,21].
- L: total $CD8^+$T cells population. These are active tumor specific cells that are part of the specific immune response. Consequently, these cells are only present in large numbers when tumor cells are present [6,21,12].
- C: number of circulating lymphocytes (or white blood cells). This number is commonly considered as a measurement of the patient health [17,16].
- M: chemotherapy drug concentration in the blood stream.
- I: immunotherapy drug concentration in the blood stream.

Before going further into the model description, it is important to underline that, as it is recalled in [6,7], *there is no universal agreement as to the underlying dynamics or the precise cascades of events that take place in the immune response process.* The model recalled and described below is however based on published statements derived from clinical validations [8,9,22] as well as on reasonable assumptions depicted on Table 1. It is worth recalling however that the model is not used in the derivation of the control law, but only in the validation step.

The considerations and assumptions depicted on Table 1 lead to the following simplified model for cells population dynamics in presence of tumor cells and under mixed immune and chemotherapy medical interventions [6]:

The number of tumor cells grows logistically in the absence of immune response.	$aT(1-bT)$ in the r.h.s of (1)
Both NK and CD8$^+$T kill tumor cells.	$-cNT$ and $-DT$ in the r.h.s of (1)
The cytokine IL-2 stimulates the recruitment of CD8$^+$T cells [21]. It is naturally present in the immune system but it can also be injected therapeutically [12]. The additional amount of cytokine IL-2 that corresponds to this medical intervention is represented by the state variable I.	$\frac{p_I I}{g_I + I} L$ in the r.h.s of (6)
NK cells are normally present in the body even in the absence of tumor cells. In the model of [6], the source of NK cells is taken to be a fraction of the circulating lymphocytes. This is clearly a simplification that aims to represent a rather complex cascade of biological events that result in the stimulation of NK cells production.	eC n the r.h.s of (2)
The fraction of cells (both tumor and healthy cells) killed by chemotherapy depends on the amount of drug present in the body.	$(1-e^{-M})$ in the r.h.s of (1)-(4)
Both the NK and the CD8$^+$T cell populations are stimulated by the presence of tumor cells.	$g\frac{T^2}{h+T^2}N$ and $j\frac{D^2T^2}{k+D^2T^2}L$ in (2) and (3) respectively
All cells are in competition for space and nutriments.	bilinear terms NT, LT, NL^2 in equations (1)-(3)

Table 1
Table describing the modeling assumptions and their mathematical formulations. This Table has to be related to the system dynamics described by (1)-(7)

$$\frac{dT}{dt} = aT(1-bT) - cNT - DT - K_T(1-e^{-M})T, \tag{1}$$

$$\frac{dN}{dt} = eC - fN + g\frac{T^2}{h+T^2}N - pNT - K_N(1-e^{-M})N, \tag{2}$$

$$\frac{dL}{dt} = -mL + j\frac{D^2T^2}{k+D^2T^2}L - qLT + (r_1N + r_2C)T - \\ -uNL^2 - K_L(1-e^{-\frac{M}{5}})L + \frac{p_I I}{g_I + I}L + v_L(t), \tag{3}$$

$$\frac{dC}{dt} = \alpha - \beta C - K_C(1 - e^{-M})C, \tag{4}$$

$$\frac{dM}{dt} = -\gamma M + v_M(t), \tag{5}$$

$$\frac{dI}{dt} = -\mu_I I + v_I(t) \tag{6}$$

$$D = d\frac{(L/T)^l}{s + (L/T)^l} \tag{7}$$

To summarize, the model involves 6 state variables T, N, L, C M, and I, and 3 manipulated (control) variables v_M, v_L and v_I. The model involves 24 parameters: $a, b, c, d, s, K_T, e, f, g, h, K_N, m, j, k, q$, r_1, r_2, u, K_L, α, β, K_C, γ and l. In [6], two sets of experimentally identified parameters for two different patients are given. These sets, unknown to the controller, are used in the remainder of the paper for simulation and validation purposes.

3 Formulations of optimal control problems for mixed therapy

The basic paradigm in cancer therapy drug administration is to decrease the number of tumor cells T while monitoring the number of circulating lymphocytes C as they are a good measurement of the patient health [11,13,19,3]. To express these concerns, two different formulations of optimal control problems can be used:

(1) The first formulation is the one used by [19,15,1,4] among many other works. It amounts to minimize the tumor size $T(t_f)$ at the end of some prediction horizon while keeping the circulating lymphocytes above a given threshold

$$\mathcal{P}_1 : \min_{v_M(\cdot), v_L(\cdot), v_I(\cdot)} T(t_f) \quad \text{under } C(t) \geq C_{min},\ \forall t \in [0, t_f] \tag{8}$$

This formulation aims to reduce the tumor size as fast as possible under the health constraint $C(t) \geq C_{min}$.

(2) The second possible formulation, proposed in [4], uses a more careful approach. Namely, it aims to maximize the patient health under a contraction constraint on the tumor size at the end of the prediction horizon. More precisely, the following game is defined:

$$\mathcal{P}_2 : \max_{v_M(\cdot),v_L(\cdot),v_I(\cdot)} \min_{t\in[0,t_f]} C(t) \quad \text{under } T(t_f) \leq \gamma T(0) \text{ with } \gamma \in]0,1[\tag{9}$$

This formulation focuses on the *health level* by accepting probably a slower decrease of the tumor size.

In both formulations, the decision inputs are the drug injections, namely, the chemotherapy drug injection v_M and the two immunotherapy drugs injections v_I and v_L. Therefore a feedback treatment strategy is an algorithm that computes on-line the suitable injections v_M, v_L and v_I based on past measurements of the patient's two key quantities: the number of tumor cells T and the number of circulating lymphocytes C. Particularly, a model-free strategy is a strategy in which, the above algorithm does not involve any a-priori knowledge on the dynamic model that underlines the cells populations evolution.

4 The proposed model-free feedback strategy

As explained in the preceding section, in order to define a feedback injection strategy, one has to compute the injection quantities v_M, v_L and v_I as functions of the past measurements of T and C. It is shown in this section that a qualitative difference holds between the chemotherapy treatment on one side and the immunotherapy treatment on the other side since the chemotherapy drug induces opposite effects that involve a trade-off to be computed by optimization while the immunotherapy induces direct and always beneficial effects and can therefore be handled more easily.

Let $\tau_s > 0$ be a sampling period, the decision instants denoted by $\{t_k = k.\tau_s\}_{k=1}^{N}$ correspond to the instants at which the plannified injection strategy is updated. The goal of immunotherapy is to strengthen the ability of the body to fight against cancer by enhancing the effectiveness of the patient immune system. Its action does only produce beneficial effect unlike chemotherapy that induces positive effects (tumor regression) and negative effects (regression of the immune system). As a result, the strategy of immunotherapy will only be based on the evolution of the tumor cells population, whereas chemotherapy will depend on both tumor cells population and circulating lymphocytes populations.

More precisely, the immunotherapy feedback law expresses the following simple rules:

(1) Injections are positive and upper bounded by some saturation levels:

$$0 \leq v_L \leq v_L^{max} \quad ; \quad 0 \leq v_I \leq v_I^{max} \tag{10}$$

where in accordance with [6], a maximum TIL's boost of $v_L^{max} = 10^9$ cells and a maximum IL-2 boost of $v_I^{max} = 5 \times 10^5$ cells are considered.

(2) Injections are fired when the tumor cells population is not SUFFICIENTLY decreasing, namely:

$$\Big\{\delta T(k) = T(k) - T(k-1) \geq -\delta_{max} \cdot T(k)\Big\} \Rightarrow \text{Injection} \tag{11}$$

(3) when injections are fired, the injection level depends on the tumor cells populations. In particular, it vanishes when T goes to 0.

The above rules can be summarized through the following explicit expressions that completely define the immunotherapy feedback

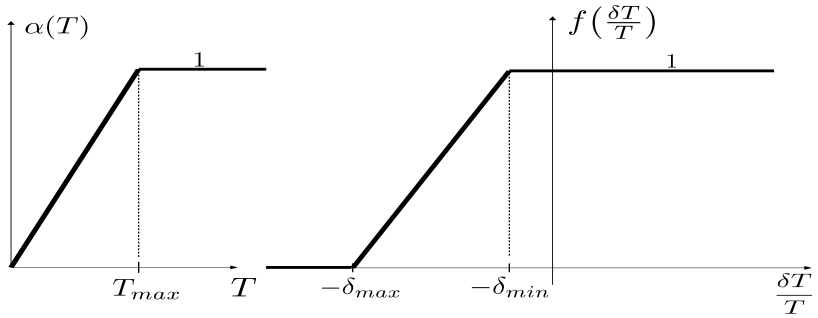

Fig. 1. Definition of the maps $\alpha(\cdot)$ and $f(\cdot)$ involved in the immunotherapy feedback strategy defined by (12)-(13).

law:

$$v_L(T, \delta T) = \left[\alpha(T) \cdot f(\frac{\delta T}{T})\right] \cdot v_L^{max} \tag{12}$$

$$v_I(T, \delta T) = \left[\alpha(T) \cdot f(\frac{\delta T}{T})\right] \cdot v_I^{max} \tag{13}$$

where the functions $\alpha(\cdot)$ and $f(\cdot)$ are those depicted on Figure 1.

4.2 The chemotherapy feedback law

As pointed out earlier, unlike immunotherapy that has only a beneficial action, chemotherapy induces beneficial effects (tumor regression) together with harmful effects (regression of the immune system). This creates the need for a trade-off in the chemotherapy dosage and the best choice can be computed by on-line optimization. However, the optimization requires the consequences of each choice on the cost function to be predicted and this needs a prediction model. Since we aim to develop a (biological model)-free feedback law, the prediction model has to be computed on line and exclusively from past measurement data. In order to do this, we first impose the following structure of the chemotherapy injection over a sampling period $[k\tau_s, (k+1)\tau_s]$:

$$v_M(t) = \begin{cases} 0 & \text{if } t \in [k\tau_s, (k+\frac{1}{2})\tau_s] \\ v_M(k) & \text{otherwise} \end{cases}$$

where $v_M(k)$ is the decision variable (chemotherapy injection during the time interval $[(k+\frac{1}{2})\tau_s, (k+1)\tau_s]$) to be computed by optimization. More precisely, the injection $v_M(k)$ is computed as follows:

(1) Note first that one disposes of the following past measurements that have been acquired during the past sampling period $[(k-1)\tau_s, k\tau_s]$:

$$v_M(k-1) \quad , \quad T(k-1) \quad , \quad T(k-\frac{1}{2}) \quad , \quad T(k)$$

(2) Note also that the value $T(k-\frac{1}{2})$ results from $T(k-1)$ when applying no chemotherapy injection ($v_M = 0$) during half a sampling period $\tau_s/2$.

(3) Moreover, the value $T(k)$ results from $T(k-\frac{1}{2})$ when applying the chemotherapy injection $v_M = v_M(k-1)$ during half the sampling period $\tau_s/2$.

(4) Using the above two facts, it is possible to identify a short term affine prediction model that takes the following form:

$$\dot{T}_p = a_{k-1} + b_{k-1} v_M(k) \tag{14}$$

where the coefficients a_{k-1} and b_{k-1} are identified using the preceding sampling period related measurements by:

$$a_{k-1} = \frac{2}{\tau_s}[T(k-\frac{1}{2}) - T(k-1)] \tag{15}$$

$$b_{k-1} = \frac{2}{(v_M(k-1)+\nu)\tau_s}[T(k) - 2T(k-\frac{1}{2}) + T(k-1)] \tag{16}$$

where $\nu > 0$ is a regularization coefficient.

(5) Similarly, based on the measurements:

$$v_M(k-1) \quad , \quad C(k-1) \quad , \quad C(k-\frac{1}{2}) \quad , \quad C(k)$$

it is possible to identify an approximate affine prediction model for the circulating lymphocytes:

$$\dot{C}_p = g_{k-1} + h_{k-1} v_M(k) \tag{17}$$

in which g_{k-1} and h_{k-1} have the same expressions as a_{k-1} and b_{k-1} respectively provided that T is replaced by C in (15) and (16).

(6) At the decision instant $k\tau_s$, the prediction models (14)-(17) are used to predict the future evolutions of the tumor size and the circulating lymphocytes level for each candidate value of the chemotherapy injection v_M over some prediction horizon $\tau_p = N_p\tau_s$. More precisely, for all future instant $(k+i)\tau_s$ over the prediction horizon $[k\tau_s, (k+N_p)\tau_s]$, the prediction is given by:

$$T_p(k+i, v_M) = \left[e^{a_{k-1} i\tau_s}\right] T(k) + \left[(1 - e^{a_{k-1}\tau_s/2}) \cdot b_{k-1} \cdot i\right] v_M \tag{18}$$

$$C_p(k+i, v_M) = \left[e^{g_{k-1} i\tau_s}\right] T(k) + \left[(1 - e^{g_{k-1}\tau_s/2}) \cdot h_{k-1} \cdot i\right] v_M \tag{19}$$

The predictions are clearly exclusively constructed based on the past measurements and are based on simple models that can be directly used to derive *sub-optimal* solutions (if any) to the optimal control problems $\mathcal{P}_1$ and/or $\mathcal{P}_2$. Note that when performing the corresponding optimization, the following quantized set of admissible values for the chemotherapy injections is used:

$$v_M \in \{0, 0.2, 0.4, 0.6, 0.8, 1\} \cdot v_M^{max}$$

where v_M^{max} is the maximum allowable chemotherapy dosage.

As for the choice of the optimal control problem to be used, the idea is to focus primarily on the second optimal control problem $\mathcal{P}_2$, namely the one that tries to maximize the patient health under a contraction constraint on the predicted level of the tumor size at the end of the prediction horizon of length $\tau_p = N_p\tau_s$. If there is no solution to this optimal control problem, the constrained optimal control problem $\mathcal{P}_1$ is used in order to enforce the decrease of the tumor cell under health constraint.

In both cases, the resulting solution $v_M(k)$ is applied over the second half of the sampling period $[k\tau_s, (k+1)\tau_s]$. The corresponding measurements are used to compute the updated values of the model parameters, namely a_k, b_k, g_k and h_k and a new prediction model is obtained that is used to formulate the new two approximated optimal control problems $\mathcal{P}_1$ and $\mathcal{P}_2$ and the procedure is repeated. Note that this corresponds to an NMPC control scheme since a prediction over a rather long horizon is used to compute an optimal sequence, only the first part of this optimal sequence is applied on the present sampling period at the end of which a new optimal sequence is computed based on an updated model, the fist part of it is applied and so on.

5 Simulation results

The set of parameters used in the validating simulations corresponds to the patient 9 of [6]. The parameters used in the proposed feedback and the initial conditions are given in Table 2.
The simulation results for a strategy based on a single treatment (immunotherapy or chemotherapy) with an initial tumor size of $T_0 = 9.10^7$ cells are shown in Figure 2. The strategies obtained for a single drug (chemotherapy on Figure 2 (a) or immunotherapy on Figure 2 (b)) are unsuccessful since they do not lead to a tumor regression.

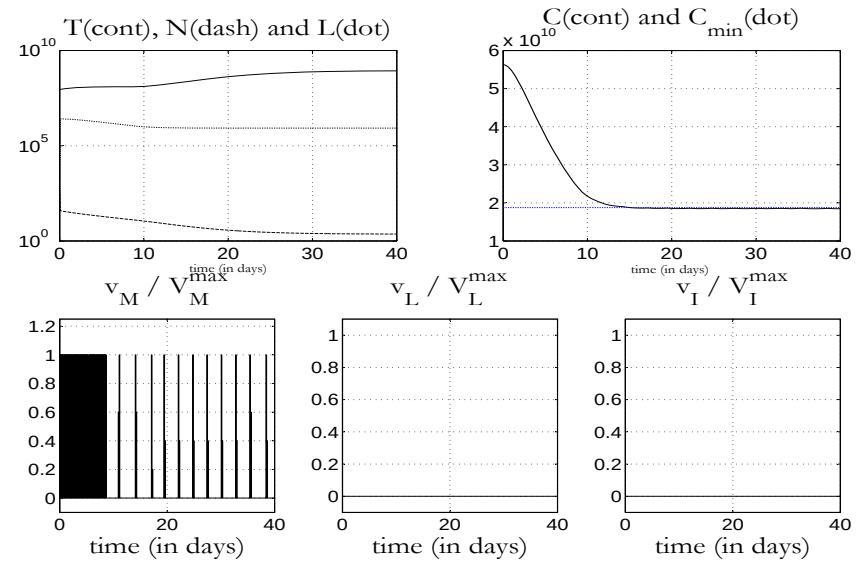

(a)

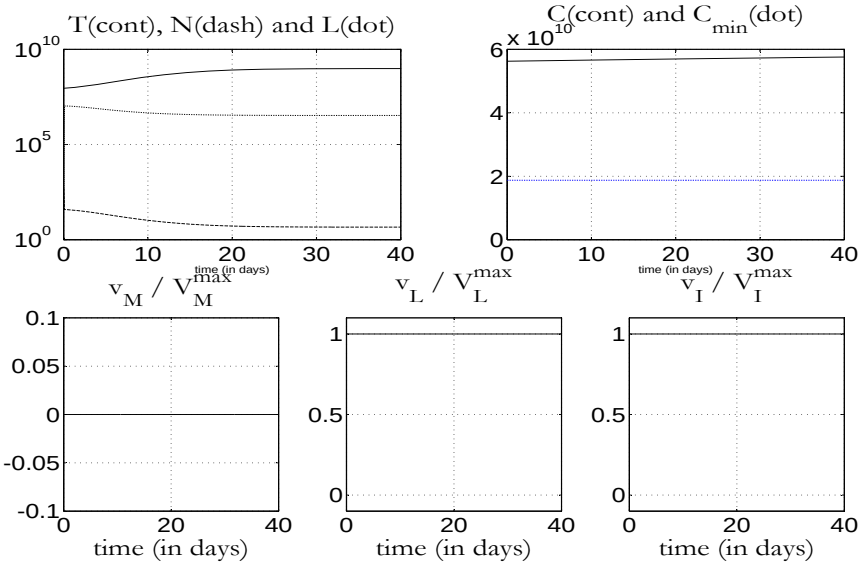

(b)

Fig. 2. Behavior of the population levels using a single treatment, in Figure (a) only chemotherapy is used and in Figure (b) only immunotherapy is used. The strategies based on a single drug are unsuccessful since they do not lead to a tumor regression. [Simulation conditions: $T_0 = 9 \times 10^7$ cells, $\tau_p = 48h$, combined use of optimal control problems $\mathcal{P}_1$ and $\mathcal{P}_2$ with on Figure (a) exclusively chemotherapy and on Figure (b) exclusively immunotherapy]

On the other hand we can observe on Figure 3, that the mixed strategy is successful leading to a tumor regression while during all the treatment, the population of circulating lymphocytes

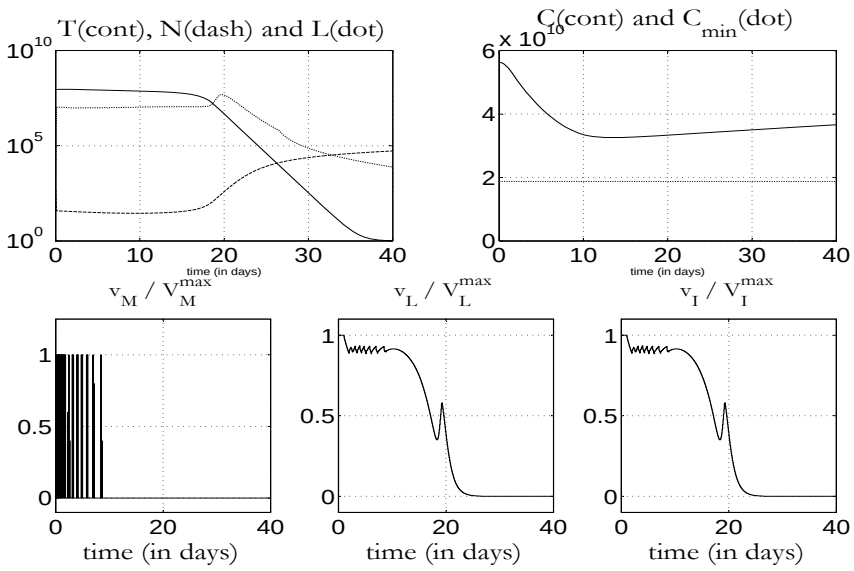

Fig. 3. Successful treatment leading to a tumor regression while maintaining a high population level of circulating lymphocytes. This simulation when compared to that of Figure 2 shows the relevance of the combined therapy. [Simulation conditions: $T_0 = 9 \times 10^7$ cells, $\tau_p = 48h$, combined use of optimal control problems $\mathcal{P}_1$ and $\mathcal{P}_2$, with mixed immuno-chemotherapy]

is kept far above the minimum threshold of circulating lymphocytes, which witnesses good patient health. The sharp decrease of tumor cells population starts around the 10th day, this decrease is at the very beginning due to both actions of chemotherapy and immunotherapy, and then it is exclusively due to the action of immunotherapy, as a result, the population level of circulating lymphocytes is kept high above the threshold.
It is interesting to notice that the drug injection results in applying chemotherapy at the beginning of the treatment therapy. This solution is different from the optimal solutions obtained in [11,14,24] that apply the drugs at the end of the treatment period. In [1], it has been shown that the formulation $\mathcal{P}_1$ shows qualitatively different solutions that have exactly the same cost value. The solution for the compartmental model considered in these works is sensitive to the initial guess.

5.1 Influence of the choice of the optimal control problem

Let us now observe the influence of the choice of the optimal control problem. We can observe on Figure 4.(b) the results that may be obtained when only the optimal control problem $\mathcal{P}_1$ is used under the same initial conditions as in the simulation shown on Figure 3. Though the treatment is successful, we can observe that the combined use of both optimal control problems [Figure 4.(a)] ensure a high level of circulating lymphocytes at the end of the treatment period, and therefore a good patient health at the price of slower tumor regression. Note that this is achieved by stopping the chemotherapy earlier while maintining immunoterapy slightly longer.

5.2 Influence of the prediction horizon

Different values of prediction horizon lead to different evolutions of the tumor cells and circulating lymphocytes populations. Figure 5 shows the influence of the prediction horizon for two prediction horizons ; Figure 5 (a) shows the strategy obtained with a prediction horizon of 4 hours and Figure 5 (b) the strategy obtained for a prediction horizon of 48 hours. For a 4-hour prediction horizon [Figure 5 (a)], we can observe that the predictive control strategy leads to a faster decrease of both tumor cells and circulating lymphocytes (thus a lower patient health) than for a 48-hour prediction horizon [Figure 5 (b)]. This fact can be explained by the different drug strategies used in the case of a short or a long prediction horizon. As shown on Figure 5 (a), for a 4 hours prediction horizon, intensive chemotherapy is applied longer, as a result the patient health is lower. On the other hand, Figure 5 (b) shows that the strategy obtained with a prediction horizon of 48 hours use less chemotherapy and more immunotherapy, the tumor regression takes longer but the patient health is higher.
As a matter of fact, the value of the prediction horizon mod-

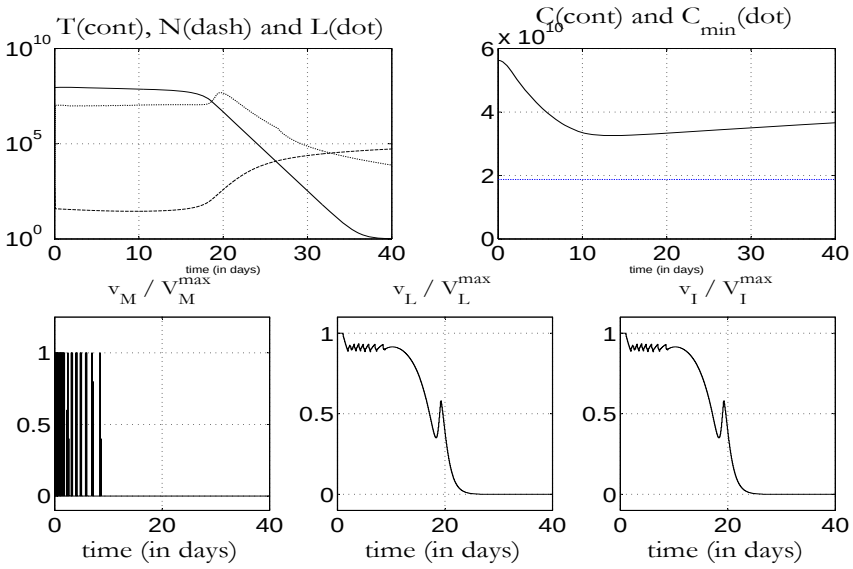

(a)

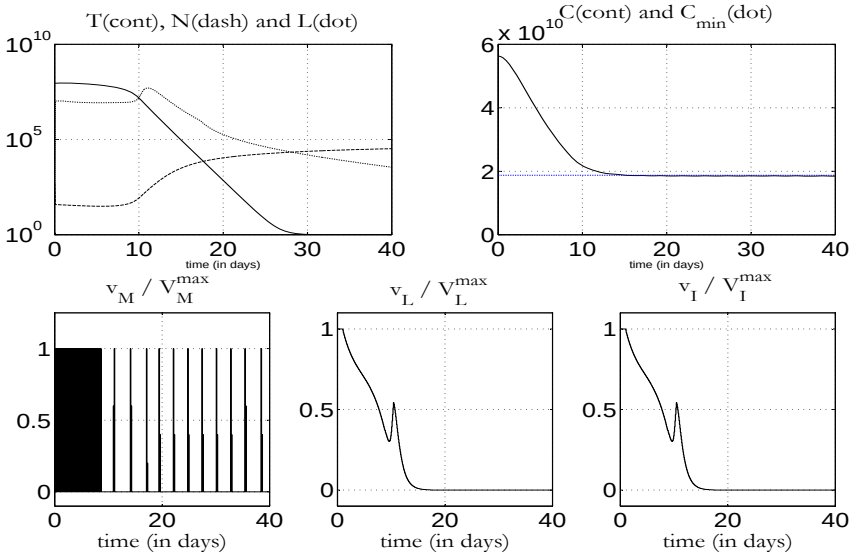

(b)

Fig. 4. Illustration of the efficiency of the switching strategy between the two optimization problems $\mathcal{P}_1$ and $\mathcal{P}_2$. Indeed, when this switching strategy is used [Figure (a)], a higher level of circulating lymphocytes is obtained at the price of a slightly slower tumor regression. Figure (b) shows the result when only problem $\mathcal{P}_1$ is used. [Simulation conditions: $T_0 = 9 \times 10^7$ cells, $\tau_p = 48h$, combined use of optimal control problems $\mathcal{P}_1$ and $\mathcal{P}_2$, with mixed immuno-chemotherapy]

ifies the optimal control problem ($\mathcal{P}_1$ or $\mathcal{P}_2$) that is chosen at each decision instant. The switching between the two optimal control problem is shown on Figure 6 (b) for different prediction

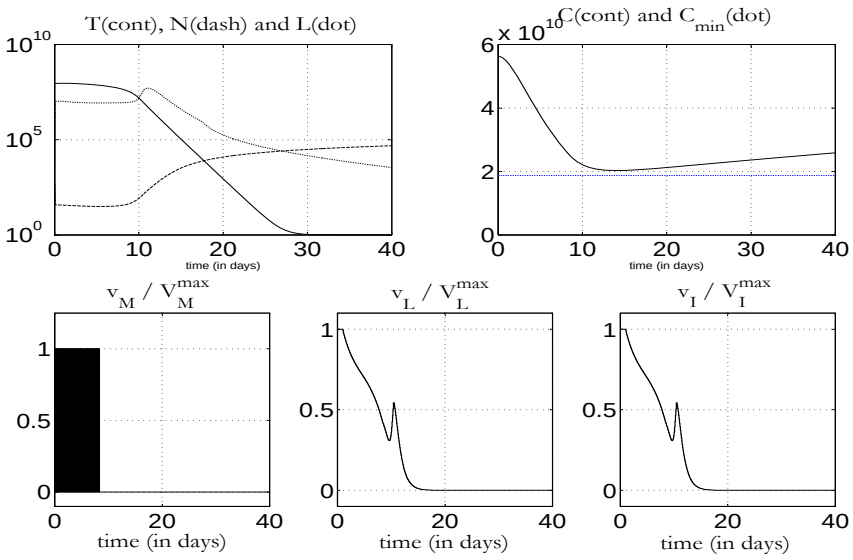

(a)

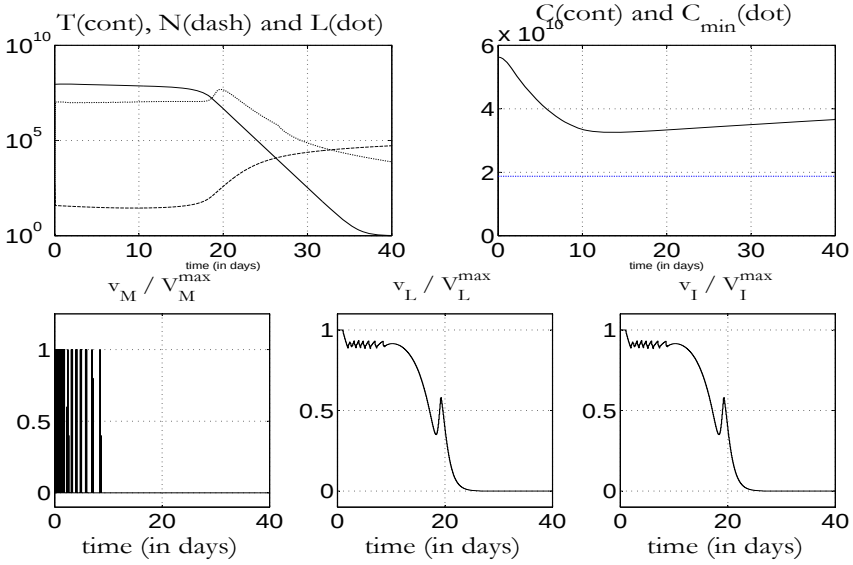

(b)

Fig. 5. Influence of the prediction horizon: (a) 4 hours (b) 48 hours. Small prediction horizons lead to extensive use of chemotherapy at the beginning of the treatment. This leads to faster tumor regression to the detriment of the patient health. [Simulation conditions: $T_0 = 9 \times 10^7$ cells, $\tau_p = 4h$, combined use of optimal control problems $\mathcal{P}_1$ and $\mathcal{P}_2$, with mixed immuno-chemotherapy.]

horizons, and Figure 6 (a) shows the corresponding evolution of tumor cells and circuating lymphocytes. For short prediction horizons, the optimal control problem $\mathcal{P}_1$ is selected longer at the beginning of the treatment. (Recall that the optimal control

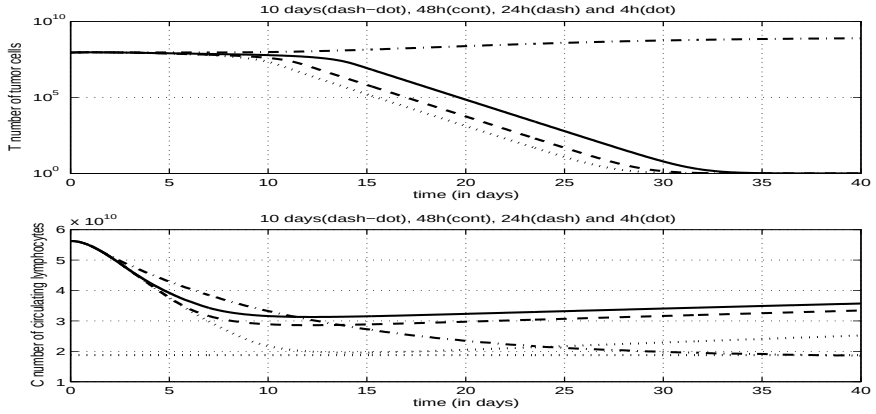

(a)

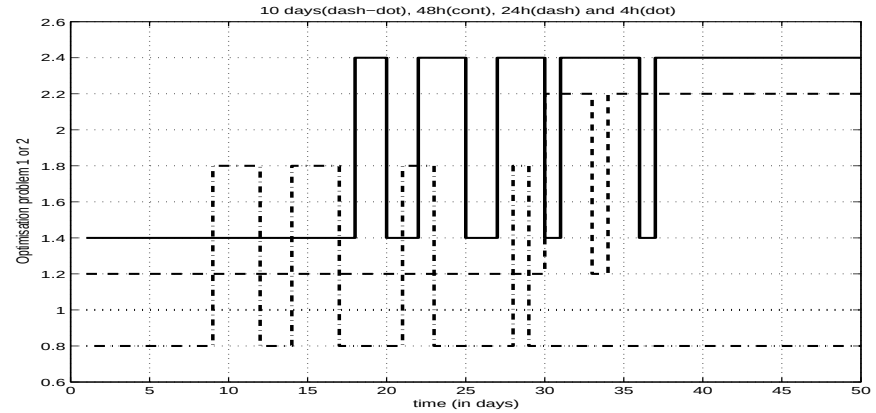

(b)

Fig. 6. (a) Behavior of the tumor cell T and circulating lymphocyte populations for four values of the prediction horizon. For short prediction horizon, the tumor cell population decreases faster, but also do the circulating lymphocytes. For large prediction horizon, the treatment fails. (b) Choice of the optimal control problem selected for each decision instant between $\mathcal{P}_1$ and $\mathcal{P}_2$. 1 stands for the choice of the optimal control problem $\mathcal{P}_1$, and 2 for the optimal control problem $\mathcal{P}_2$. [Simulation conditions: $T_0 = 9 \times 10^7$ cells, $\tau_p = \{4h, 24h, 48h, 10 \times 24h\}$, combined use of optimal control problems $\mathcal{P}_1$ and $\mathcal{P}_2$, with mixed immuno-chemotherapy]

problem $\mathcal{P}_1$ is selected when no solution satisfies the contraction factor with the optimal control problem $\mathcal{P}_2$). The contraction fac-

tor being identical for any prediction horizon, so short prediction horizons have less chances to fulfill this criterium, the optimal control problem $\mathcal{P}_1$ is thus more frequently selected. Moreover, recall that the strategy of the optimal control problem $\mathcal{P}_2$ aims at maximizing the patient health under a contraction constraint on the tumor size. As a result this strategy yields high population level of circulating lymphocytes thanks to a restricted use of chemotherapy and a more extensive use of immunotherapy. Based on these considerations, a longer prediction horizon seems a better choice since it ensures a better patient health at the price of a slightly slower tumor regression. However, we can observe on Figure 6 (a) that when the prediction horizon is too long, the model-based feedback control is not able any more to induce a tumor regression since the oversimplified prediction model becomes too erroneous.

The high sensitivity of the result to the choice of the prediction horizon suggests an on-line adaptation mechanism for the prediction horizon. More precisely, the prediction horizon has to be taken as long as possible provided that it represents faithfully the system evolution. This property can be monitored by comparing the predicted population levels with the actually measured one. Depending on the value of the error the prediction horizon is increased or decreased. Figure 7 (b) shows the evolution of the prediction horizon during the treatment period with an initial value of 10 days. Note that the bad quality of the prediction model with this initial value that induced an unsuccessful treatment [see Figure 6 (a)] has been detected by the updating scheme and the horizon has been temporarily reduced leading to a successful treatment.

6 Conclusion

This paper proposes a new approach for the drug administration in mixed cancer therapy. In order to avoid parameter uncertainties that are frequent when dealing with biological mod-

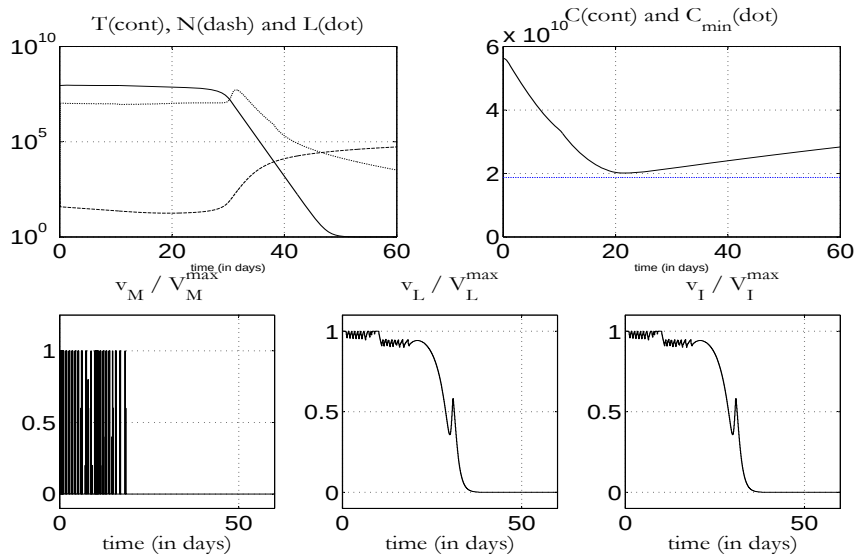

(a)

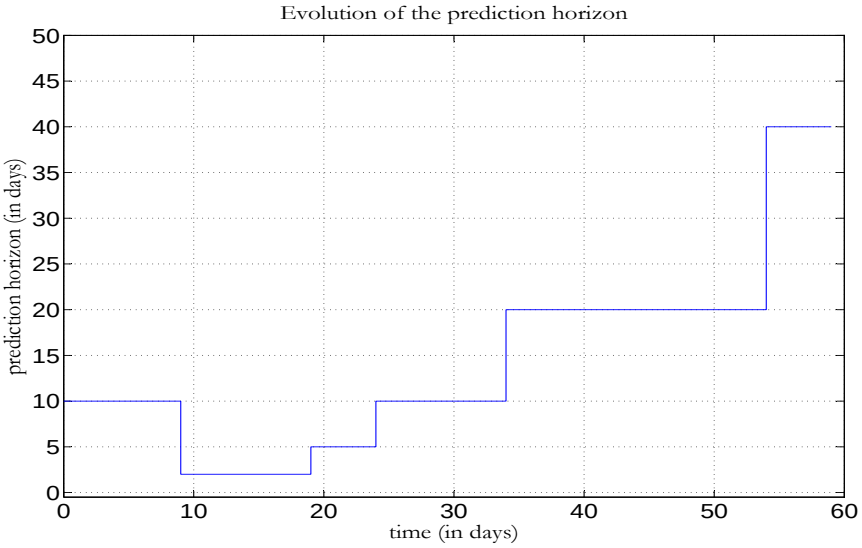

(b)

Fig. 7. Illustration of the efficiency of the prediction horizon updating strategy. (a) Evolution of the cells populations and the injected drugs starting from an initial value of the prediction horizon of 10 days under the updating strategy for the prediction horizon. (b) Corresponding evolution of the prediction horizon. Nota that the initial value of 10 days would have lead to an unsuccessful therapy as shown on Figure 6. [Simulation conditions: $T_0 = 9 \times 10^7$ cells, $\tau_{p0} = 10 \times 24h$, combined use of optimal control problems $\mathcal{P}_1$ and $\mathcal{P}_2$, with mixed immuno-chemotherapy and adaptation algorithm of τ_p.]

els, we propose here to build a model-free predictor of the key state variables based on the past measurements. The efficiency

of this strategy is illustrated through dedicated simulations. This strategy reveals particularly good performances, and thus appears very promising.

References

[1] M. Alamir and S. Chareyron. *State-Constrained Optimal Control Applied to Cell-Cycle-Specific Cancer Chemotherapy*, chapter Positive Systems, LNCIS 341. C. Commault and N. Marchand (Eds), pages 271–278. Springer-Verlag Berlin Heidelber, 2006.

[2] D. Barbolosi, G. Freyer, J. Ciccolini, and A. Iliadis. Dosage regimen optimization in cancer chemotherapy using a mathematical model. *Bulletin du cancer ISSN 0007-4551*, 90:167–175, 2003.

[3] S. Chareyron and M. Alamir. Mixed immunotherapy and chemotherapy of tumors: Feedback design and model updating schemes. Campinas, Brazil, July 16 to 20 2007. Conference on Computational and Mathematical Population Dynamics (CMPD2).

[4] S. Chareyron and M. Alamir. Mixed immunotherapy and chemotherapy of tumors: Feedback design and model updating schemes. *Journal of Theoretical Biology*, in press, 2008.

[5] L. G. de Pillis and A. E. Radunskaya. Immune response to tumor invasion. In *Bathe, K. (Ed.), Computational Fluid ans Solid Mechanics, vol. 2.* MIT Press, Cambridge, MA., 2003.

[6] L. G. dePillis, W. Gu, and A. E. Radunskaya. Mixed immunotherapy and chemotherapy of tumor: modeling, application and biological interpretations. *Journal of Theoretical Biology*, 238:841–862, 2005.

[7] L. G. dePillis, A. E. Radunskaya, and C.L. Wiseman. A validated mathematical model of cell-mediated immune response to tumor growth. *Cancer Research*, 61:7950–7958, 2005.

[8] A. Diefenbach, E.R. Jensen, A.M. Jamieson, and D. Raulet. Rael and h60 ligands of the nkg2d receptor stimulate tumor immunity. *Nature*, 413:165–171, 2001.

[9] M.E. Dudley, J.R. Wunderlich, P.F. Robbins, J.C. Yang, P. Hwu, D.J. Schwartzentruber, S.L. Topalian, R. Sherry, N.P. Restifo, A.M. Hubicki, M.R. Robinson, M. Raffeld, P. Duray, C.A. Seipp, L. Rogers-Freezer, K.E. Morton, S.A. Mavroukakis, D.E. White, and Rosenberg. S.A. Cancer regression and autoimmunity in patients after clonal repopulation with antitumor lymphocytes. *Science*, 298(5594):850–854, 2002.

[10] M. Eisen. *Mathematical Models in Cell Biology and Cancer Chemotherapy*, volume 30 of *lecture Notes in Biomath.* Springer-Verlag, New York, 1979.

[11] K. R. Fister and J. C. Panetta. Optimal control applied to cell-cycle-specific cancer chemotherapy. *SIAM Journal on Applied Mathematics*, 60 (3):1059–1072, 2000.

[12] W. C. Kirschner and J. C. Panetta. Modeling immunotherapy of the tumor-immune interaction. *J. Math. Biol.*, 37 (3):235–252, 1998.

[13] R. Martin and K. Teo. *Optimal Drug Administration in Cancer Chemotherapy.* World Scientific, Singapore, 1994.

[14] R. B. Martin. Optimal drug scheduling of cancer chemotherapy. *Automatica*, 1992.

[15] A. S. Matveev and A. V. Savkin. Application of optimal control theory to the analysis of cancer chemotherapy regimens. *Systems & Control Letters*, 46:311–321, 2002.

[16] B. Melichar, J. Dvorak, P. Jandik, M. Touskova, D. Solichova, J. Megancova, and Z. Voboril. Intraarterial chemotherapy of malignant melanoma metastatic to liver. *Hepatogastroenterology*, 48 (42):1711–1715, 2001.

[17] M. M. Mustafa, G. R. Buchanan, N. J. Winick, G. H. McCracken, I. Tkaczewski, M. Lipscomb, Q. Ansari, and M. S. Agopian. Immune recovery in children with malignancy after cessation of chemotherapy. *J. Pediatr. Hematol. Oncol.*, 20 (5)(5):451–457, 1998.

[18] J. C. Panetta. A mathematical model of breast and ovarian cancer treated with paclitaxel. *Math. Biosci.*, 146:89–113, 1997.

[19] L. G. De Pillis and A. Radunskaya. A mathematical tumor model with immune resistance and drug therapy: An optimal control approach. *Journal of Theoretical Medecine*, 3:79–100, 2001.

[20] L. G. De Pillis and A. Radunskaya. The dynamics of optimally controlled tumor model: a case study. *Mathematical and Computer Modelling*, 37(11):1221–1244, 2003.

[21] I. M. Roitt, J. Brostoff, and D. K. Male. *Immunology.* Mosby, St. Louis, 1993.

[22] A. Rosenberg, S. and M. Lotze. Cancer immunotherapy using interleukin-2 and interleukin-2-activated lymphocytes. *Annu. Rev. Immunol.*, 4:681–709, 1986.

[23] A. Swierniak and Z. Duda. Mathematical population dynamics. *Journal of Optimization Theory and Applications*, 2:347–358, 1995.

[24] A. Swierniak, U. Ledzewicz, and H. Schttler. Optimal control for a class of comportemental models in cancer chemotherapy. *Int. J. Appl. Math. Comput. Sci.*, 13 (3):357–368, 2003.

Simulation data	value
Maximum dose of immunotherapy	$v_L^{max} = 10^9$ and $v_I^{max} = 5 \times 10^5$
Maximum dose of chemotherapy	$v_M^{max} = 1$
contraction factor	$\gamma = 0.9$
Circulating lymphocytes threshold	$C_{min} = 1.8750.10^{10}$
Constants for the feedback law on immunotherapy [see Figure 1]	$\delta_{max} = 1.0 \times 10^6$, $\delta_{min} = 0.0$ and $T_{max} = 1.0 \times 10^7$
Initial conditions	$L_0 = 50$, $N_0 = 5 \times 10^2$ $C_0 = 3 \times C_{min}$

Table 2
The set of parameters used in the control strategy